

# PRESTO-Tango as an open-source resource for interrogation of the druggable human GPCRome

Wesley K Kroeze<sup>1,2,5</sup>, Maria F Sassano<sup>1,2,5</sup>, Xi-Ping Huang<sup>1,2,5</sup>, Katherine Lansu<sup>1</sup>, John D McCorvy<sup>1</sup>, Patrick M Giguère<sup>1</sup>, Noah Sciaky<sup>1</sup> & Bryan L Roth<sup>1-4</sup>

**G protein-coupled receptors (GPCRs) are essential mediators of cellular signaling and are important targets of drug action. Of the approximately 350 nonolfactory human GPCRs, more than 100 are still considered to be ‘orphans’ because their endogenous ligands remain unknown. Here, we describe a unique open-source resource that allows interrogation of the druggable human GPCRome via a G protein-independent  $\beta$ -arrestin-recruitment assay. We validate this unique platform at more than 120 nonorphan human GPCR targets, demonstrate its utility for discovering new ligands for orphan human GPCRs and describe a method (parallel receptorome expression and screening via transcriptional output, with transcriptional activation following arrestin translocation (PRESTO-Tango)) for the simultaneous and parallel interrogation of the entire human nonolfactory GPCRome.**

GPCRs are proteins that contain seven transmembrane helices and are capable of transducing a wide variety of extracellular stimuli into intracellular signals mediated by G proteins from four groups ( $G_s$ ,  $G_i$ ,  $G_{12}$  or  $G_{13}$ , and  $G_q$ ) as well as by arrestins and other effectors<sup>1</sup>. The human genome encodes more than 350 different nonolfactory GPCRs and a similar number of olfactory GPCRs<sup>2-4</sup>. In addition to acting as signal transducers, GPCRs are the targets for more than one-third of currently prescribed medications<sup>5,6</sup>. Approximately one-third of the nonolfactory GPCRs in the human genome are orphan GPCRs, whose endogenous or natural ligands are unknown<sup>2-4</sup>, whereas many more have been inadequately interrogated with respect to their ligands. Thus, much of the druggable GPCRome—like other drug-target families such as the kinome<sup>7</sup>—represents ‘dark matter’ of the human genome. Because many of these sparsely annotated GPCRs will probably represent fruitful future therapeutic targets, identifying drug-like chemical leads for the entire family of druggable GPCRs represents a major goal for chemical biology. Unfortunately, interrogating the druggable GPCRome *en masse* in a parallel and simultaneous fashion is currently technologically and economically unfeasible.

The difficulty in screening the entire druggable GPCRome in parallel is due mainly to the inherent diversity of signal-transduction cascades, which renders attempts at parallel profiling challenging. Thus, for instance, functional assays for the identification of agonists at orphan and other sparsely annotated GPCRs have typically used readouts that depend on the native or forced<sup>1</sup> coupling of GPCRs with G proteins, e.g.,  $G_s$ ,  $G_i$ ,  $G_q$ ,  $G_{12}$  or  $G_{13}$  (refs. 8–14). Unfortunately, these approaches are not well suited for the parallel and simultaneous genome-wide interrogation of the druggable GPCRome<sup>1</sup>. Alternatively, measurement of G protein-independent  $\beta$ -arrestin recruitment

provides a feasible and universal assay platform because nearly all tested GPCRs can induce arrestin translocation<sup>15,16</sup> (Supplementary Table 1). A wide variety of approaches have been described to quantify GPCR- $\beta$ -arrestin interactions, including high-content screening (HCS)<sup>17</sup>, bioluminescence resonance energy transfer (BRET)<sup>18</sup>, enzyme complementation<sup>19</sup> and transcriptional activation following arrestin translocation (Tango)<sup>20</sup>, although none are routinely performed in a genome-wide, parallel manner. As we show here, the Tango approach has a number of advantages for high-throughput assays, including its independence from G protein coupling, its generally high signal-to-background ratios and its amplification of relatively small initial inputs into large readout signals. Independence from G protein coupling facilitates interrogation of orphan GPCRs, whose coupling partners are unknown. Some of the advantages of the Tango assay might also be shared by other readout systems, including, for example, assays for changes in impedance or dynamic mass redistribution (reviewed in ref. 21). Indeed, arrestin recruitment may be part of the dynamic mass-redistribution response measured in receptor-expressing cells responding to agonists, as suggested, but not directly shown, by the results of a previous study<sup>22</sup>. Our goal was to develop the Tango assay into a platform that could encompass the entire druggable GPCRome. Although our assay does not differ substantially from the Tango assay<sup>20</sup> in terms of the general concept, several notable changes including the design of the plasmid constructs and the assay execution have distinct advantages, as we describe below. We also demonstrate a method, PRESTO-Tango, that facilitates the rapid, efficacious, parallel and simultaneous profiling of biologically active compounds across essentially the entire human druggable GPCRome. Additionally, we document how our approach leads to the easy identification of new

<sup>1</sup>Department of Pharmacology, University of North Carolina, Chapel Hill, Chapel Hill, North Carolina, USA. <sup>2</sup>National Institute of Mental Health Psychoactive Drug Screening Program, University of North Carolina, Chapel Hill, Chapel Hill, North Carolina, USA. <sup>3</sup>Program in Neuroscience, University of North Carolina, Chapel Hill, Chapel Hill, North Carolina, USA. <sup>4</sup>Division of Chemical Biology and Medicinal Chemistry, University of North Carolina, Chapel Hill, Chapel Hill, North Carolina, USA. <sup>5</sup>These authors contributed equally to this work. Correspondence should be addressed to B.L.R. (bryan\_roth@med.unc.edu).

Received 21 December 2014; accepted 25 March 2015; published online 20 April 2015; doi:10.1038/nsmb.3014

synthetic and naturally occurring agonists for orphan GPCRs. Finally, because our platform is open source, our methods and reagents are freely available to the scientific community.

## RESULTS

### Rationale and design

We sought to develop a platform suitable for the parallel and simultaneous interrogation of every nonfactory druggable GPCR in the human genome. Accordingly, we devised a ‘modular’ design strategy to produce a Tango construct for each GPCR, extensively modifying the previously described design of the Tango assay<sup>20</sup> (general scheme in Fig. 1a). The underlying principle was to make each GPCR construct in such a way that various ‘modules’ could be conveniently included or excluded as desired (Fig. 1a). At the 5′ end, we included a cleavable signal sequence to promote membrane localization<sup>23</sup> and a Flag epitope tag to allow monitoring of cell-surface expression by immunohistochemistry. At the 3′ end, we included the sequences for the tobacco etch virus nuclear inclusion endopeptidase (TEV)-cleavage site and the tetracycline transactivator (tTA) protein, exactly as previously published<sup>20</sup>. We then codon-optimized GPCR sequences for expression in human cell lines and added sequence from the C terminus of the V<sub>2</sub> vasopressin receptor (V<sub>2</sub> tail) after each receptor sequence, to promote arrestin recruitment<sup>20,24–26</sup>. The receptor sequence and the V<sub>2</sub> tail were flanked by restriction sites to allow easy excision or subcloning of other targets at those sites as well as more efficient gene synthesis. We designed the codon-optimized sequences to exclude their flanking restriction sites. Additionally, it should be noted that by simple mutagenesis to insert a stop codon at the 3′ end of the receptor sequence, these Tango constructs can also be used in other functional assays; i.e., they can be ‘de-Tango-ized’.

The sequence of an entire prototypical Tango construct is given in **Supplementary Note 1**, and the sequences of all of the receptor inserts produced can be found online (<https://pdspdb.unc.edu/prestotango/>). When multiple splicing isoforms existed for a given GPCR, we used the longest or the most prevalent form for the Tango constructs. We excluded a few GPCRs with extremely long N termini and a few

that could not be expressed in *Escherichia coli*, generating a total of 315 synthetic Tango-ized GPCRs (**Supplementary Table 2**).

### Validation of the PRESTO-Tango platform

In preliminary experiments, we transfected each Tango-ized construct and then examined anti-Flag immunofluorescence for both total and surface expression (examples in Fig. 1b). Of 315 constructs examined, 302 (96%) were surface expressed (**Supplementary Table 2**). Of the remaining GPCRs that were not efficiently surface expressed, receptor expression could be visualized in permeabilized cells (data not shown).

To test the utility of the platform, we assayed nearly all of the non-orphan receptors for activation by their canonical agonists. In total, we attempted to validate 167 nonorphan GPCRs and were successful with 125 (75%). Of the family A GPCRs, we validated 81% (summarized in **Table 1**). We also present concentration-response curves for a prototypical nonorphan GPCR, the neuromedin B receptor (NMBR; also known as the BB1 bombesin receptor) for both  $\beta$ -arrestin–recruitment activity (Fig. 1c) and G protein (calcium-release) activity (Fig. 1d). Individual concentration-response curves for every validated target are shown in **Supplementary Data Set 1**. Agonist-induced activation of the Tango-ized GPCRs resulted in variable responses ranging from about 1.3-fold above baseline to 184-fold for the MLNR motilin receptor. Importantly, we discovered ligand-induced arrestin recruitment for the first time, to our knowledge, in 23 different GPCRs, including the BB1 bombesin receptor (Fig. 1c), the CHRM5 muscarinic acetylcholine receptor (Fig. 2a), the CX3CR1 chemokine receptor (Fig. 2b), the DRD4 dopamine receptor (Fig. 2c, despite a report that this target does not interact with arrestin<sup>27</sup>), the GAL3 galanin receptor (Fig. 2d), the NMUR1 (Fig. 2e) and NMUR2 (Fig. 2f) neuromedin receptors, and others shown in **Supplementary Data Set 1**, including the AVPR1B vasopressin receptor, the CCKAR cholecystokinin receptor, the CMKOR1 orphan chemokine receptor, the GPBA bile-acid receptor (despite a report that this target does not interact with arrestin<sup>28</sup>), the HTR7 serotonin receptor, the LPAR5 lysophospholipid receptor (also known as GPR92), the MRGPRX4 orphan receptor, the NTSR2 neurotensin receptor, the P2RY13 and P2RY14 purinergic receptors,

**Figure 1** Design, principle and validation of selected Tango assays. **(a)** Top, modular design of Tango constructs. HA, hemagglutinin. Blue arrowheads, Cla I sites; green arrowheads, Age I sites. Bottom, general scheme for the  $\beta$ -arrestin (Tango) recruitment assay. Upon activation of the GPCR by an agonist (L) (1),  $\beta$ -arrestin is recruited to the C terminus of the receptor (2). This is followed by cleavage of the GPCR fusion protein at the TEV protease–cleavage site (3). Cleavage results in the release of the tTA transcription factor (4), which, after transport to the nucleus, activates transcription of the luciferase reporter gene (5). **(b)** Surface expression of two selected Tango constructs, as shown by immunofluorescence with an anti-Flag antibody. **(c,d)** Concentration-response curves of a prototypical nonorphan GPCR, the neuromedin B receptor (NMBR) stimulated by neuromedin B (NMB) in the Tango assay **(c)** and in a calcium-release assay **(d)**. EC<sub>50</sub>, half-maximal effective concentration. Data are shown as mean  $\pm$  s.e.m. of typical experiments done in quadruplicate. Curves were fitted with GraphPad Prism 5.0.

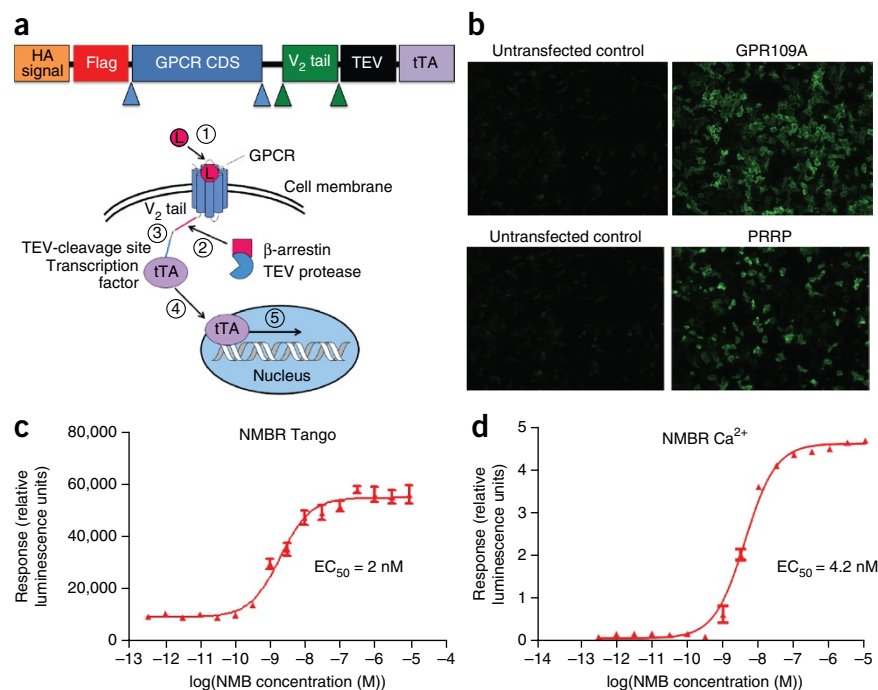


**Table 1 Assay validation statistics**

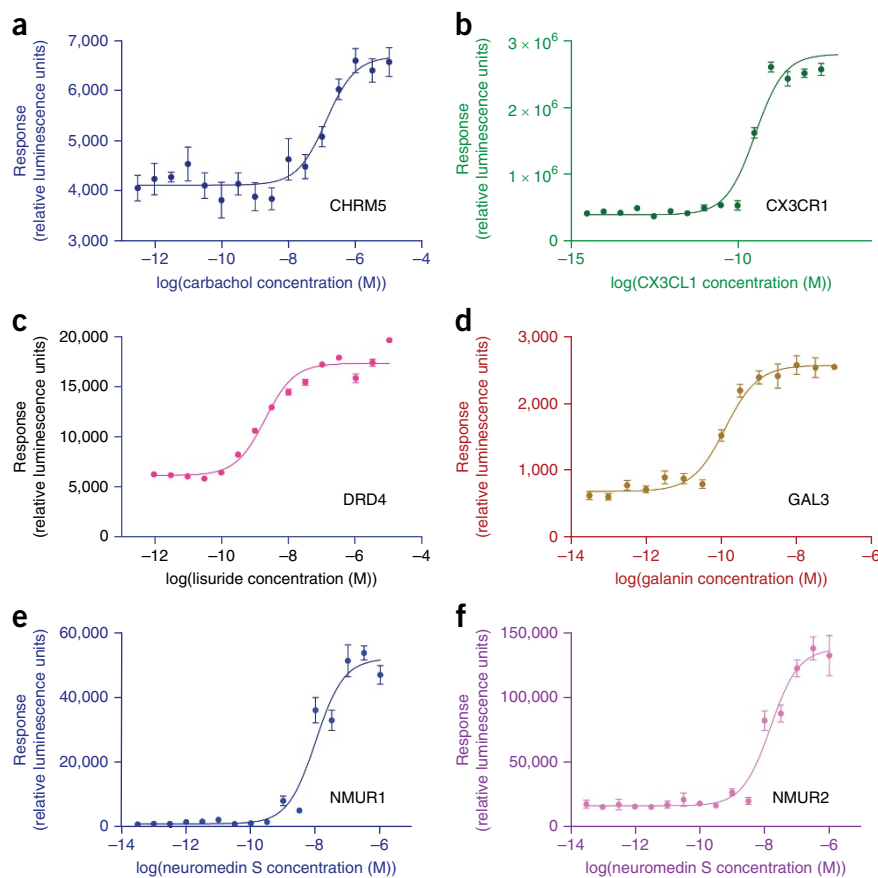
Group	Validated in this study	Could not be validated	Validation attempted	Not attempted or orphan	Total
A	127 (82%)	28 (18%)	155	110	265
B	8 (57%)	6 (43%)	14	2	16
C	0	8 (100%)	8	7	15
Adhesion	0	0	0	17	17
Other	0	0	0	2	2
Total	135 (76%)	42 (24%)	177	139	315

the PTGER1 and PTGFR (despite a report that this target does not interact with arrestin<sup>29</sup>) prostanoid receptors, the RXFP4 relaxin receptor, the S1PR2 lysophospholipid receptor, the SSTR4 somatostatin receptor (despite a report that this target does not interact with arrestin<sup>30</sup>) and the TACR2 tachykinin receptor.

Additionally, we tested whether the antagonist activity of test compounds could be quantified by simply preincubating cells with potential antagonists before agonist exposure. For instance we, like others<sup>31,32</sup>, found that neurotensin was inactive as an agonist at NTSR2 neurotensin receptors, although SR48692 and SR142948 are NTSR2 agonists (Supplementary Fig. 1a). Intriguingly, both neurotensin and the HRH1-histamine receptor antagonist levocabastine were antagonists of SR48692- or SR142948-induced arrestin-recruitment responses in NTSR2-transfected cells (Supplementary Fig. 1b,c), as reported by others using orthogonal assays<sup>31,32</sup>. Thus, these results validate the use of the Tango  $\beta$ -arrestin-recruitment assay for measurements of antagonist activity.

As noted previously, the constructs tested included the C-terminal tail of the V<sub>2</sub> vasopressin receptor in order to enhance arrestin interactions with the various receptors<sup>20,25</sup>. Notably, the presence of the V<sub>2</sub> tail has been reported to have little to no effect on the Tango assay for some receptors<sup>24</sup>. In our experience, removal of the V<sub>2</sub> tail had little effect on the ligand-induced responses of some receptors (e.g., the LTBR4 leukotriene receptor (Supplementary Fig. 1d)), increased the ligand-induced responses of others (e.g., the CMKLR1 chemerin receptor (Supplementary Fig. 1e)) and decreased the ligand-induced responses of others (e.g., the FFAR2 free-fatty-acid receptor (GPR43; Supplementary Fig. 1f)). A systematic and complete study of the effects of including or excluding the V<sub>2</sub> tail remains to be done, though our results (Supplementary Fig. 1d–f) provide a path forward for further optimization of the Tango assay.

**Figure 2** Demonstration of arrestin mobilization with the Tango assay. (a–f) Concentration-response curves for the response of the CMRM5 muscarinic acetylcholine receptor to carbachol ( $EC_{50} = 133.8$  nM,  $n = 4$ ) (a), the CX3CR1 chemokine receptor to its ligand CX3CL1 ( $EC_{50} = 0.34$  nM,  $n = 4$ ) (b), the DRD4 dopamine receptor to lisuride ( $EC_{50} = 2.0$  nM,  $n = 3$ ) (c), the GAL3 galanin receptor to galanin ( $EC_{50} = 0.13$  nM,  $n = 4$ ) (d), the NMUR1 neuromedin receptor to neuromedin S ( $EC_{50} = 10.2$  nM,  $n = 4$ ) (e) and the NMUR2 neuromedin receptor to neuromedin S ( $EC_{50} = 15.4$  nM,  $n = 4$ ) (f). Data are shown as mean  $\pm$  s.e.m. of technical replicates.



In additional experiments, we also validated the Tango assay in ‘antagonist mode’ by determining the effect of preexposure of GPCR-expressing cells to 1  $\mu$ M clozapine on their responses to the agonist lysergic acid diethylamide (LSD). For some targets, clozapine had little or no effect on the responses of cells to LSD, e.g., the HTR1A and HTR1D serotonin receptors (Supplementary Fig. 2a,b). For others, e.g., the HTR1B serotonin receptor and the ADRA2B adrenergic receptor (Supplementary Fig. 2c,d), the major effect of clozapine on LSD concentration-response curves was to shift them to the right. For still other GPCRs, e.g., the HTR1E, HTR1F, HTR2A and HTR5 serotonin receptors, and the DRD2 dopamine receptor, the effect of clozapine was to both shift the curves to the right and to decrease the maximal effective concentration ( $E_{max}$ ) (Supplementary Fig. 2e–i). These results therefore further validate the use of the Tango  $\beta$ -arrestin-recruitment assay in antagonist mode and thus facilitate the discovery of new modes of action of pharmacological agents.

Next, we tested each of the Tango-ized constructs for constitutive activity, i.e., recruitment of arrestin in the absence of known ligands (as detailed in Online Methods, and as seen in Supplementary Fig. 3, Supplementary Table 3 and Fig. 3a,b). Constitutive activity varied over a range of more than about 500-fold among the various GPCRs; in one set of GPCRs tested, the ratio of the maximal to the minimal luminescence was 437, and in another, the ratio was 551 (Supplementary Table 3 and Fig. 3a,b). Detailed analyses revealed no readily apparent sequence-encoded pattern upon comparison of GPCRs with high and low constitutive activity, although we note that several members of the serotonin and purinergic receptor families had relatively high constitutive activity as compared to the activity of the other tested GPCRs.

**Figure 3** Constitutive (or basal) activity for Tango-ized constructs. (a,b) Data for the orphan and peptide GPCRs (a) and the nonorphan (b) GPCRs ( $n = 4$  for each target), shown as mean  $\pm$  s.e.m. of technical replicates.

We also discovered that although our standard protocols specify overnight incubation with ligands (Online Methods), very brief exposures to ligand (i.e., 15 min) are sufficient to stimulate measurable responses in the Tango assay, although overnight incubation is apparently required for maximum signal amplification (Supplementary Fig. 4). This feature facilitates testing of compounds that may be toxic to cells at long exposure but that may reveal activity at GPCR targets at short exposure. Additional studies suggest that the minimum incubation time for robust observation of responses to agonists in the Tango assay depends on the target being tested but that, for screening purposes, 1–2 h is generally sufficient, provided that the signal is amplified overnight (data not shown). Thus, optimization of agonist exposure time may improve assay performance depending on the individual targets or ligands to be studied.

#### 'Many target-few compound' parallel GPCRome screening

Conventional small molecule-based screening often involves testing of hundreds of thousands of compounds at a single target, and, as we have demonstrated previously (PubChem BioAssay AID 588463), Tango assays are useful for such conventional 'one-target-at-a-time' GPCR screening. An alternative and potentially innovative approach, which we have named PRESTO-Tango, is to screen collections of perturbants (e.g., small molecules, peptides, short interfering RNAs, clustered regularly interspaced short palindromic repeats (CRISPR)-based editing constructs and so on) against the druggable human GPCRome in a simultaneous fashion. Although simultaneous interrogation of the entire druggable GPCRome is clearly important, it has not been feasible for both technical and economic reasons. Once we developed a resource containing most of the druggable GPCRs, we wondered

whether they could be screened in a 384-well format in a simultaneous and parallel fashion (Fig. 4a, Online Methods and detailed description of the technology in Supplementary Note 2). For an initial validation, we screened the hallucinogen LSD and the selective serotonin reuptake inhibitor fluoxetine against 133 nonorphan, nonolfactory GPCR targets (Supplementary Note 3). LSD displayed activity at 15 of the tested targets, including several unexpected ones such as the  $\alpha_{2B}$  adrenergic receptor and the D<sub>4</sub> and D<sub>5</sub> dopamine receptors (Fig. 4b–d). Fluoxetine, which has been reported to have few 'off targets'<sup>33</sup>, showed modest agonist activity at the SSTR3 somatostatin receptor, which we could not confirm in follow-up assays (data not shown), thus supporting its selectivity for the serotonin transporter and not for any GPCR targets.

#### New activities in the GPCRome

Given our initial success with two highly annotated small molecules and well-known GPCRs, we next determined whether we could expand this approach by screening a collection of approved drugs (NIH Clinical Collection of compounds, NCC-1 library; <http://nihsmr.evotec.com/evotec/sets/ncc>) against 91 orphan and poorly annotated GPCRs (heat map of results in Fig. 5a; entire data set in Supplementary Table 4). Some of the tested drugs displayed promiscuous inhibitory activity (Fig. 5a and Supplementary Table 4). Thus, for example, resveratrol produced a reduction greater than two-fold at 70 of 91 targets (77%) and homoharringtonine at 58 of 91 targets (64%); 12 additional compounds produced a reduction in luminescence greater than two-fold at 20 or more of the 91 targets tested. This sort of inhibition could be due to cytotoxicity, compound aggregation or inhibition of the luciferase reporter<sup>34</sup>. In contrast, a few others—most notably the aminopeptidase inhibitor bestatin (increase of more than two-fold at 59 of 91 targets tested (65%))—induced increased

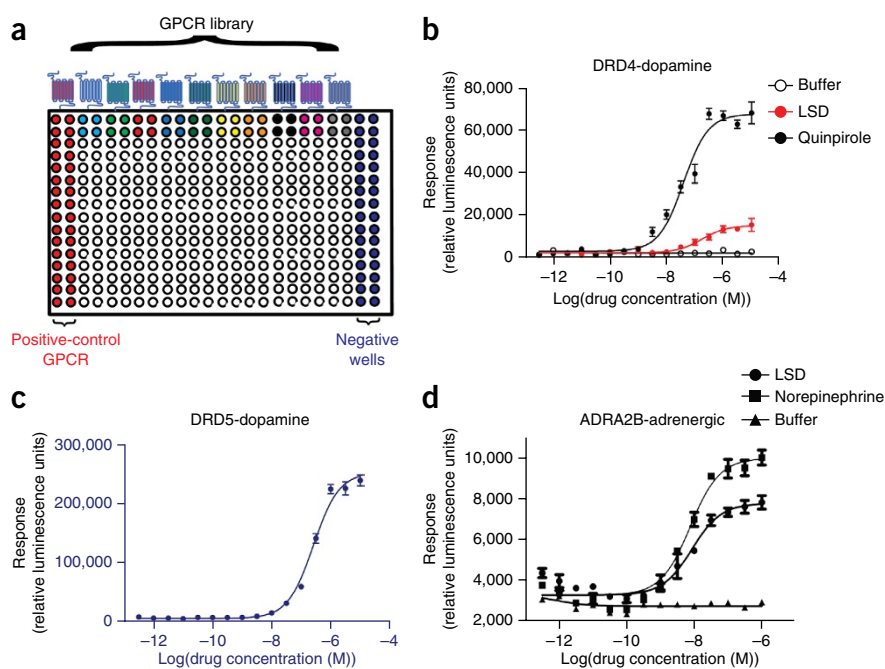


**Figure 4** Compound profiling with the PRESTO-Tango method at the human GPCRome. (a) General assay format, in which compounds are screened against a large number of GPCRs in quadruplicate in 384-well plates; for clarity only the first row of individual GPCRs is shown. (b–d) Concentration-response curves of LSD at various targets: DRD4-dopamine (b), DRD5-dopamine (c) and ADRA2B-adrenergic (d). Data are shown as mean  $\pm$  s.e.m. of 3 (in d–f) or 4 (in c) technical replicates, and curves were fitted with GraphPad Prism. Experiments in d were repeated twice.

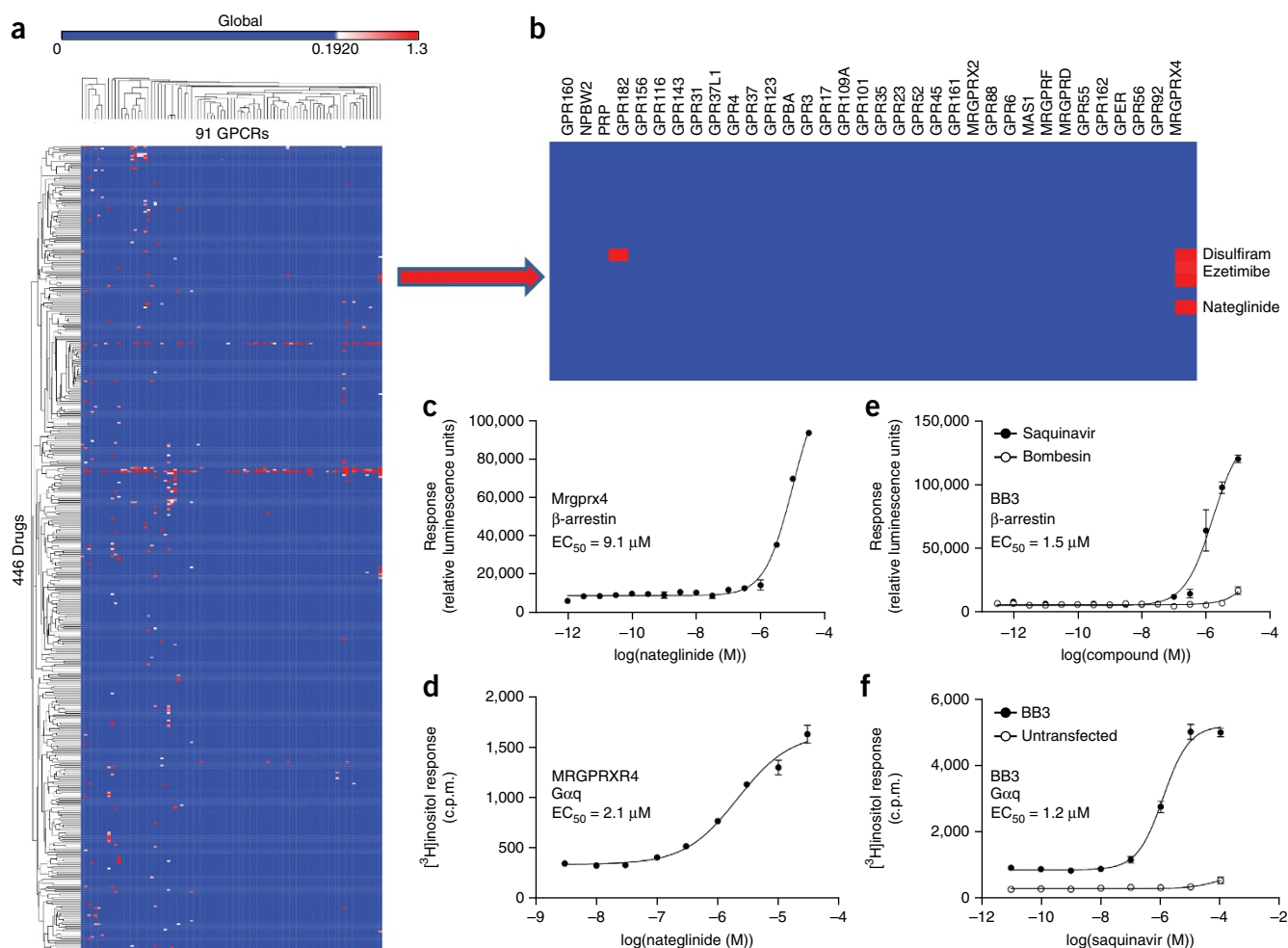


**Figure 5** New ligand-target interactions detected by parallel GPCRome screening. Results of screening of the 446-compound NCC-1 library at 91 GPCR targets in the Tango assay and follow-up studies are shown. (a) Heat map of the entire matrix (red, stimulation of luminescence over background). (b) Close-up view of a section of the heat map in a, showing the activity of nateglinide at MRGPRX4. (c) Concentration-response curve of nateglinide at MRGPRX4 in the Tango assay ( $n = 4$ ). (d) Concentration-response curve of nateglinide at MRGPRX4 by PI hydrolysis ( $n = 3$ ). (e) Concentration-response curve of saquinavir at the BB3 bombesin receptor in the Tango assay ( $n = 4$ ). (f) Concentration-response curve of saquinavir at the BB3 bombesin receptor by PI hydrolysis ( $n = 3$ ). Data in c–f are shown as mean  $\pm$  s.e.m. of technical replicates.

activity. Although we did not investigate the mechanism for this promiscuous agonist effect, such promiscuous activity has been previously ascribed to enhanced luciferase stability<sup>35,36</sup>. These results illustrate the value of screening at multiple targets simultaneously and in a parallel fashion, enabling the separation of false-positive ‘frequent hitters’ from screening hits that can be productively pursued.

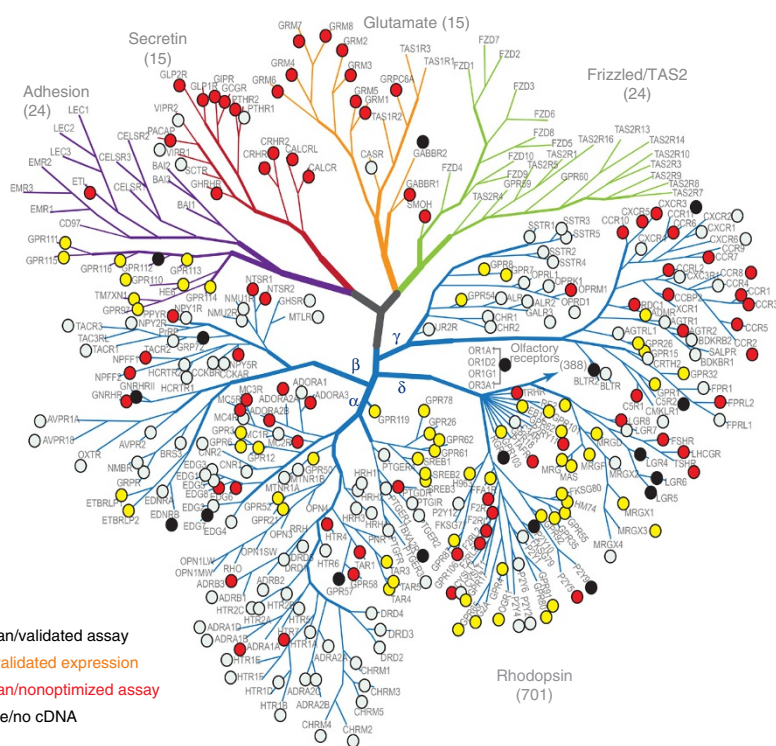
Among the most intriguing activities revealed by our screen of 446 compounds at 91 targets (i.e., 40,586 compound-target tests) was the activity of the  $K_{ATP}$ -channel blocker nateglinide at the MRGPRX4 orphan GPCR (Fig. 5b and Supplementary Table 4). Nateglinide induced a 45-fold increase in luminescence over basal levels in the initial screen, and, of the 91 targets tested, nateglinide was apparently selective for only one target, MRGPRX4 (Fig. 5b and Supplementary Table 4). We subsequently confirmed the concentration-dependent activity of nateglinide at MRGPRX4 by Tango (Fig. 5c) and phosphatidylinositol (PI)-hydrolysis assays (Fig. 5d). Nateglinide had only modest activity at high concentrations when we measured cyclic AMP at MRGPRX4, and it was inactive at MRGPRX1, MRGPRX2 or MRGPRX3 (Supplementary Fig. 5a). The magnitude of the cAMP response was much lower than the response to isoproterenol in MRGPRX4-expressing cells, a result due to the responses of the

constitutively expressed  $\beta_2$  adrenergic receptor in human embryonic kidney (HEK) cells (Supplementary Fig. 5b). These data, combined with the inability of nateglinide to inhibit a cAMP response to isoproterenol in these cells (Supplementary Fig. 5c), and the activity of nateglinide in the PI-hydrolysis assay (Fig. 5d), indicate for the first time, to our knowledge, that MRGPRX4 is primarily a  $G_q$ -coupled receptor. Next, we prepared stably expressing cell lines for MRGPRX1, MRGPRX2 and MRGPRX4 receptors; calcium-mobilization assays performed with these cell lines showed concentration-dependent responses of MRGPRX1-expressing cells to the cognate ligand BAM8-22 (Supplementary Fig. 6a,b), of MRGPRX2-expressing cells to SB 205607 (Supplementary Fig. 6c,d) and of MRGPRX4-expressing cells to nateglinide (Supplementary Fig. 6e,f), results further indicating that this group of receptors is primarily  $G_q$  coupled in HEK cells.

In preliminary screening studies, we also identified the HIV protease inhibitor saquinavir as a potential agonist at an orphan GPCR, the so-called BB3 bombesin receptor. To further investigate saquinavir’s BB3 activity, and to validate the specificity of our platform, we confirmed its concentration dependence at BB3 (Fig. 5e) and showed that the related bombesin receptors BB1 (Supplementary Fig. 7a) and BB2 (Supplementary Fig. 7b) were insensitive to saquinavir

**Figure 6** Tango-izing the druggable GPCRome.

Tree-based phylogram of the nonolfactory GPCRome showing the status of the Tango assay for each GPCR. Cyan circles represent nonorphan GPCRs for which assays were validated; yellow circles represent assays for which expression of orphan GPCRs were validated; blue circles represent nonorphan GPCRs for which optimized assays are not yet available; and black circles represent GPCRs for which no Tango-ized construct is available. Slashes denote 'with'. GPCR-network diagram is adapted with permission from ref. 49, Elsevier.



in the Tango assay. In orthogonal calcium-mobilization assays, saquinavir did not stimulate a response in BB1- or BB2-expressing cells (**Supplementary Fig. 7c,d**) but did stimulate a response in BB3-expressing cells (**Supplementary Fig. 7e**), and we also confirmed this activity by an assay of PI hydrolysis (**Fig. 5f**). Thus, these data confirm that saquinavir has substantial off-target activity at the BB3 orphan GPCR and validate that the apparent target specificity of the Tango assay can be recapitulated in orthogonal assays.

Our initial screen of the NCC-1 library also included the related target MRGPRX2 (**Supplementary Table 4**), at which the most active compounds included the  $\delta$ -opioid-receptor agonist SB 205607 (also known as TAN-67), confirming results from a prior report<sup>37</sup>. Interestingly, two other opioids, levorphan and dextromethorphan, as well as the antihistaminergic and antiserotonergic compound cyproheptadine, the antihistaminergic compound ketotifen and the antiserotonergic compound pizotyline, also showed activity in the Tango assay at MRGPRX2 (**Supplementary Table 4**)—all of which we confirmed in concentration-response studies (**Supplementary Fig. 8a**). We also confirmed the concentration-dependent activities of SB 205607 and dextromethorphan at MRGPRX2 by PI hydrolysis (**Supplementary Fig. 8b**). An intriguing discovery was the finding that the  $\kappa$ -opioid receptor-selective antagonist JD1c and the selective salvinorin A analog RB64 displayed substantial activity at MRGPRX2 in the Tango assay (**Supplementary Fig. 8c**).

## DISCUSSION

Here we provide PRESTO-Tango, the first open-source resource for the parallel and simultaneous interrogation of the druggable GPCRome (summarized in **Fig. 6**). Our development of this unique platform was facilitated by modifying and expanding an arrestin-recruitment (Tango) assay<sup>20</sup> for GPCR activation that is sensitive, easily executed and amenable to both HTS and simultaneous parallel screening at many GPCRs. Because knowledge of the G protein partners of each GPCR is not required, this assay is particularly suitable for 'first-pass' screening of compound libraries and for identifying ligands of orphan receptors, as has been previously suggested<sup>20,37</sup>. Importantly, we have demonstrated that: (i) activation of the majority of GPCRs can be measured with the Tango arrestin-recruitment assay; (ii) the Tango assay can also be used for measurement of antagonist activity when canonical or newly discovered agonists are available; and (iii) the simultaneous parallel screening of a few compounds with the PRESTO-Tango approach, or the parallel screening of compound libraries with the Tango method, reveals new activities

for known drugs and compounds and identifies new ligands for both sparsely annotated and orphan GPCRs. Although the Tango  $\beta$ -arrestin-recruitment assay has previously been used by many others, including us, for the DRD2 dopamine receptor<sup>38</sup>, the  $\delta$ -opioid<sup>39</sup> and  $\kappa$ -opioid<sup>40,41</sup> receptors and several serotonin receptors<sup>42</sup>, the present study is, to our knowledge, the first to adapt it to almost the entire nonolfactory GPCRome and to make the entire resource publicly available to the scientific community. This resource is thus likely to find widespread use by structural biologists who focus on GPCRs, chemical biologists intent on deconstructing the actions of drug-like compounds, molecular biologists searching for GPCR perturbants, and molecular pharmacologists and systems biologists.

Although this unique resource and the overall approach that we used are both quite powerful, the resource is currently limited by our inability to validate assays for some GPCRs. Why assays for these particular GPCRs (**Fig. 6**) could not be validated remains largely unknown, although it is likely that upon further optimization, useful assays for many of these could be perfected. Alternatively, it is conceivable that some receptors do not interact with arrestins in an agonist-dependent fashion, as has been claimed for the  $\alpha_{1A}$  adrenergic receptor (ADRA1A)<sup>43</sup>, the AT<sub>2</sub> angiotensin II receptor (AGTR2)<sup>44</sup> and the D<sub>4</sub> dopamine receptor (DRD4) (ref. 27, for example). Indeed, for the  $\beta_3$  adrenergic receptor (ADRB3), which lacks the consensus sequences for GRK phosphorylation and thus for arrestin binding, downstream signaling appears to proceed by direct interaction with kinases in the extracellular signal-regulated kinase (ERK) pathway<sup>45</sup>. For other GPCRs, for which receptor-arrestin interactions have been reported in the literature (**Supplementary Table 1**) but for which we were not able to initially validate assays, it may be that the Tango assay requires further optimization, perhaps by removal of the V<sub>2</sub> tail, or that the other arrestin-recruitment assays used in the literature are more tractable than the Tango assay for these particular GPCRs. Interestingly, there were also a few targets for which the Tango assay proved suitable, although there have been reports in the literature that

these targets did not interact with arrestin; these included the GPBA bile-acid receptor<sup>28</sup>, the prostaglandin F2 $\alpha$  (PTGFR) receptor<sup>29</sup>, the SS2R4 somatostatin receptor<sup>30</sup> and the aforementioned DRD4-dopamine receptor. It is also possible that some of the targets that could not be validated in our study interact with other members of the arrestin family but not the  $\beta$ -arrestin2 as used here. To adapt our realization of the Tango assay to interactions with other members of the arrestin family, all that would be required would be the creation of a cell line expressing alternative  $\beta$ -arrestins. Importantly, our validation studies revealed several previously undescribed agonist-induced receptor-arrestin interactions; these included at least 23 different receptor targets (Table 1 and Supplementary Data Set 1). Finally, and importantly, for some GPCR targets, e.g., the HTR5 serotonin receptor, these assays are the first reliable functional assays for receptor activation to be reported, to our knowledge. All of the validated Tango assays, and all of those that could not be validated, are summarized in Supplementary Table 5.

In addition to providing a resource for testing the function of nearly the entire druggable human GPCRome, we have also devised a method by which one or a few compounds can be tested at all 315 GPCR targets simultaneously and in parallel. Our preliminary results, in which we tested two compounds against 133 targets, showed new activities for a well-known compound, LSD, and verified the relative selectivity of the SSRI fluoxetine. Such simultaneous and parallel screening also facilitates the identification of promiscuous compounds (i.e., frequent hitters), thereby minimizing futile follow-up studies.

We also screened a small library of US Food and Drug Administration-approved drugs at 91 different GPCR targets with the Tango platform. Our intention was: (i) to discover ligands at poorly annotated or orphan receptors; (ii) to discover new targets for known drugs; (iii) to test whether the activity of compounds in the Tango assay could be confirmed in orthogonal assays; and (iv) to demonstrate the value of massively parallel screening to separate promiscuous compounds from new ligand-receptor pairs. Among the most striking results from this screen (Fig. 5b–d and Supplementary Table 4) was the remarkable activity shown by the diabetes drug nateglinide, a K<sub>ATP</sub>-channel blocker, at MRGPRX4, a member of the MAS-related GPCR family. There are four MRGPRX receptors in the human genome, and they have been reported to be expressed only in primates, with expression largely limited to the dorsal horn of the spinal cord (reviewed in ref. 46). For the most part, the MRGPRX family is thought to be peptidergic, although a few small-molecule ligands have also been reported<sup>46</sup>. By analogy to the larger family of MAS-related GPCRs, which has been extensively studied in rodents, MRGPRX receptors are thought to have a role in pain and itch<sup>46</sup>. Thus, it is interesting that the itch-inducing compound chloroquine activates MAS-related GPCRs in mice<sup>47</sup> and that rash, itching and urticaria have been reported as occasional side effects of nateglinide treatment<sup>48</sup>. Our initial screen of the NCC-1 library also revealed a large number of compounds belonging to a variety of pharmacological classes that were active at MRGPRX2, including the  $\delta$ -opioid-receptor agonist SB 205607, as previously reported<sup>37</sup>. Some other opioid-receptor ligands were also active at MRGPRX2, and this may reflect the role of similar receptors in pain<sup>46</sup>. We identified many other potential ligand-orphan GPCR pairings in the initial screen, and these will be important to pursue in subsequent studies.

Importantly, the results of our validation studies demonstrate that our approach facilitates the simultaneous profiling of hundreds of GPCRs in a cost-effective and robust manner. Additionally, as many new GPCR-ligand interactions are revealed, we have begun to illuminate a previously unknown and hidden pharmacology for known

drugs and new ligands at orphan and nonorphan GPCRs. Because this is an open-source resource, ([www.addgene.org/gpcr/roth](http://www.addgene.org/gpcr/roth)) this platform should be of immense value to the scientific community.

## METHODS

Methods and any associated references are available in the [online version of the paper](#).

*Note: Any Supplementary Information and Source Data files are available in the online version of the paper.*

## ACKNOWLEDGMENTS

This work was supported by US National Institutes of Health grant R01DA27170 (B.L.R., M.F.S. and W.K.K.) and UO1MH104974 (B.L.R., W.K.K., M.F.S. and K.L.), the US National Institute of Mental Health Psychoactive Drug Screening Program (B.L.R., M.F.S., W.K.K. and X.-P.H.) and the Michael Hooker Distinguished Professorship (B.L.R.). K.L. was supported by the University of North Carolina Department of Pharmacology Training Program (NIH 5-T32-GM007040). The authors thank R. Stevens and S. Katrich for allowing us to use and modify their GPCRome tree (Fig. 6) from ref. 49. We thank R. Axel (Columbia University) for providing HTLA cells.

## AUTHOR CONTRIBUTIONS

B.L.R. and W.K.K. conceived the general approach; W.K.K. designed the constructs; W.K.K., M.F.S., K.L. and X.-P.H. executed and analyzed validation, profiling and confirmatory assays; J.D.M. and P.M.G. validated assays; N.S. assisted with high-content microscopy; M.F.S. designed, executed and analyzed the simultaneous profiling strategy; B.L.R., W.K.K., M.F.S., K.L. and X.-P.H. wrote the paper; B.L.R. was responsible for the overall strategy.

## COMPETING FINANCIAL INTERESTS

The authors declare no competing financial interests.

Reprints and permissions information is available online at <http://www.nature.com/reprints/index.html>.

- Allen, J.A. & Roth, B.L. Strategies to discover unexpected targets for drugs active at G protein-coupled receptors. *Annu. Rev. Pharmacol. Toxicol.* **51**, 117–144 (2011).
- Bjarnadóttir, T.K. *et al.* Comprehensive repertoire and phylogenetic analysis of the G protein-coupled receptors in human and mouse. *Genomics* **88**, 263–273 (2006).
- Fredriksson, R. & Schiöth, H.B. The repertoire of G-protein-coupled receptors in fully sequenced genomes. *Mol. Pharmacol.* **67**, 1414–1425 (2005).
- Vassilatis, D.K. *et al.* The G protein-coupled receptor repertoires of human and mouse. *Proc. Natl. Acad. Sci. USA* **100**, 4903–4908 (2003).
- Hopkins, A.L. & Groom, C.R. The druggable genome. *Nat. Rev. Drug Discov.* **1**, 727–730 (2002).
- Rask-Andersen, M., Masuram, S. & Schiöth, H.B. The druggable genome: evaluation of drug targets in clinical trials suggests major shifts in molecular class and indication. *Annu. Rev. Pharmacol. Toxicol.* **54**, 9–26 (2014).
- Edwards, A.M. *et al.* Too many roads not taken. *Nature* **470**, 163–165 (2011).
- Coward, P., Chan, S.D., Wada, H.G., Humphries, G.M. & Conklin, B.R. Chimeric G proteins allow a high-throughput signaling assay of G<sub>i</sub>-coupled receptors. *Anal. Biochem.* **270**, 242–248 (1999).
- Eglen, R.M., Bosse, R. & Reisine, T. Emerging concepts of guanine nucleotide-binding protein-coupled receptor (GPCR) function and implications for high throughput screening. *Assay Drug Dev. Technol.* **5**, 425–451 (2007).
- Emkey, R. & Rankl, N.B. Screening G protein-coupled receptors: measurement of intracellular calcium using the fluorometric imaging plate reader. *Methods Mol. Biol.* **565**, 145–158 (2009).
- Hill, S.J., Williams, C. & May, L.T. Insights into GPCR pharmacology from the measurement of changes in intracellular cyclic AMP: advantages and pitfalls of differing methodologies. *Br. J. Pharmacol.* **161**, 1266–1275 (2010).
- Liu, B. & Wu, D. Analysis of the coupling of G12/13 to G protein-coupled receptors using a luciferase reporter assay. *Methods Mol. Biol.* **237**, 145–149 (2004).
- Rodrigues, D.J. & McLoughlin, D. Using reporter gene technologies to detect changes in cAMP as a result of GPCR activation. *Methods Mol. Biol.* **552**, 319–328 (2009).
- Siehl, S. & Guerini, D. Novel GPCR screening approach: indirect identification of S1P receptor agonists in antagonist screening using a calcium assay. *J. Recept. Signal Transduct. Res.* **26**, 549–575 (2006).
- Lefkowitz, R.J. & Shenoy, S.K. Transduction of receptor signals by beta-arrestins. *Science* **308**, 512–517 (2005).
- Roth, B.L. & Marshall, F.H. NOBEL 2012 Chemistry: studies of a ubiquitous receptor family. *Nature* **492**, 57 (2012).
- Barak, L.S., Ferguson, S.S., Zhang, J. & Caron, M.G. A beta-arrestin/green fluorescent protein biosensor for detecting G protein-coupled receptor activation. *J. Biol. Chem.* **272**, 27497–27500 (1997).

18. Angers, S. *et al.* Detection of beta 2-adrenergic receptor dimerization in living cells using bioluminescence resonance energy transfer (BRET). *Proc. Natl. Acad. Sci. USA* **97**, 3684–3689 (2000).
19. Yan, Y.X. *et al.* Cell-based high-throughput screening assay system for monitoring G protein-coupled receptor activation using beta-galactosidase enzyme complementation technology. *J. Biomol. Screen.* **7**, 451–459 (2002).
20. Barnea, G. *et al.* The genetic design of signaling cascades to record receptor activation. *Proc. Natl. Acad. Sci. USA* **105**, 64–69 (2008).
21. Fang, Y., Li, G. & Ferrie, A.M. Non-invasive optical biosensor for assaying endogenous G protein-coupled receptors in adherent cells. *J. Pharmacol. Toxicol. Methods* **55**, 314–322 (2007).
22. Hennen, S. *et al.* Decoding signaling and function of the orphan G protein-coupled receptor GPR17 with a small-molecule agonist. *Sci. Signal.* **6**, ra93 (2013).
23. Guan, X.M., Kobilka, T.S. & Kobilka, B.K. Enhancement of membrane insertion and function in a type IIIb membrane protein following introduction of a cleavable signal peptide. *J. Biol. Chem.* **267**, 21995–21998 (1992).
24. Hanson, B.J. *et al.* A homogeneous fluorescent live-cell assay for measuring 7-transmembrane receptor activity and agonist functional selectivity through beta-arrestin recruitment. *J. Biomol. Screen.* **14**, 798–810 (2009).
25. Kim, K.M. & Caron, M.G. Complementary roles of the DRY motif and C-terminus tail of GPCRS for G protein coupling and beta-arrestin interaction. *Biochem. Biophys. Res. Commun.* **366**, 42–47 (2008).
26. Vrecl, M. *et al.* Beta-arrestin-based Bret2 screening assay for the “non”-beta-arrestin binding CB1 receptor. *J. Biomol. Screen.* **14**, 371–380 (2009).
27. Cho, D.I., Beom, S., Van Tol, H.H., Caron, M.G. & Kim, K.M. Characterization of the desensitization properties of five dopamine receptor subtypes and alternatively spliced variants of dopamine D2 and D4 receptors. *Biochem. Biophys. Res. Commun.* **350**, 634–640 (2006).
28. Jensen, D.D. *et al.* The bile acid receptor TGR5 does not interact with beta-arrestins or traffic to endosomes but transmits sustained signals from plasma membrane rafts. *J. Biol. Chem.* **288**, 22942–22960 (2013).
29. Goupil, E. *et al.* Biasing the prostaglandin F2 $\alpha$  receptor responses toward EGFR-dependent transactivation of MAPK. *Mol. Endocrinol.* **26**, 1189–1202 (2012).
30. Tulipano, G. *et al.* Differential beta-arrestin trafficking and endosomal sorting of somatostatin receptor subtypes. *J. Biol. Chem.* **279**, 21374–21382 (2004).
31. Richard, F., Barroso, S., Martinez, J., Labbe-Jullie, C. & Kitabgi, P. Agonism, inverse agonism, and neutral antagonism at the constitutively active human neurotensin receptor 2. *Mol. Pharmacol.* **60**, 1392–1398 (2001).
32. Vita, N. *et al.* Neurotensin is an antagonist of the human neurotensin NT2 receptor expressed in Chinese hamster ovary cells. *Eur. J. Pharmacol.* **360**, 265–272 (1998).
33. Keiser, M.J. *et al.* Predicting new molecular targets for known drugs. *Nature* **462**, 175–181 (2009).
34. Auld, D.S. *et al.* Characterization of chemical libraries for luciferase inhibitory activity. *J. Med. Chem.* **51**, 2372–2386 (2008).
35. Auld, D.S., Thorne, N., Maguire, W.F. & Inglesse, J. Mechanism of PTC124 activity in cell-based luciferase assays of nonsense codon suppression. *Proc. Natl. Acad. Sci. USA* **106**, 3585–3590 (2009).
36. Auld, D.S., Thorne, N., Nguyen, D.T. & Inglesse, J. A specific mechanism for nonspecific activation in reporter-gene assays. *ACS Chem. Biol.* **3**, 463–470 (2008).
37. Southern, C. *et al.* Screening beta-arrestin recruitment for the identification of natural ligands for orphan G-protein-coupled receptors. *J. Biomol. Screen.* **18**, 599–609 (2013).
38. Allen, J.A. *et al.* Discovery of beta-arrestin-biased dopamine D2 ligands for probing signal transduction pathways essential for antipsychotic efficacy. *Proc. Natl. Acad. Sci. USA* **108**, 18488–18493 (2011).
39. Fenalti, G. *et al.* Molecular control of  $\delta$ -opioid receptor signalling. *Nature* **506**, 191–196 (2014).
40. White, K.L. *et al.* Identification of novel functionally selective kappa-opioid receptor scaffolds. *Mol. Pharmacol.* **85**, 83–90 (2014).
41. Wu, H. *et al.* Structure of the human  $\kappa$ -opioid receptor in complex with JDTC. *Nature* **485**, 327–332 (2012).
42. Wacker, D. *et al.* Structural features for functional selectivity at serotonin receptors. *Science* **340**, 615–619 (2013).
43. Stanasila, L., Abuin, L., Dey, J. & Cotecchia, S. Different internalization properties of the alpha1a- and alpha1b-adrenergic receptor subtypes: the potential role of receptor interaction with beta-arrestins and AP50. *Mol. Pharmacol.* **74**, 562–573 (2008).
44. Turu, G. *et al.* Differential beta-arrestin binding of AT1 and AT2 angiotensin receptors. *FEBS Lett.* **580**, 41–45 (2006).
45. Cao, W. *et al.* Direct binding of activated c-Src to the beta 3-adrenergic receptor is required for MAP kinase activation. *J. Biol. Chem.* **275**, 38131–38134 (2000).
46. Solinski, H.J., Gudermann, T. & Breit, A. Pharmacology and signaling of MAS-related G protein-coupled receptors. *Pharmacol. Rev.* **66**, 570–597 (2014).
47. Liu, Q. *et al.* Sensory neuron-specific GPCR Mrgprs are itch receptors mediating chloroquine-induced pruritus. *Cell* **139**, 1353–1365 (2009).
48. Twaites, B., Wilton, L.V., Layton, D. & Shakir, S.A. Safety of nateglinide as used in general practice in England: results of a prescription-event monitoring study. *Acta Diabetol.* **44**, 233–239 (2007).
49. Kritch, V., Cherezov, V. & Stevens, R.C. Diversity and modularity of G protein-coupled receptor structures. *Trends Pharmacol. Sci.* **33**, 17–27 (2012).

## ONLINE METHODS

**Transfections.** All transfections were done with an optimized calcium phosphate method<sup>50</sup>.

**'Standard' arrestin-recruitment assay.** HTLA cells (a HEK293 cell line stably expressing a tTA-dependent luciferase reporter and a  $\beta$ -arrestin2-TEV fusion gene) were a gift from the laboratory of R. Axel and were maintained in DMEM supplemented with 10% FBS, 100 U/ml penicillin and 100  $\mu$ g/ml streptomycin, 2  $\mu$ g/ml puromycin and 100  $\mu$ g/ml hygromycin B in a humidified atmosphere at 37 °C in 5% CO<sub>2</sub>. For transfection, cells were plated at  $9 \times 10^6$  to  $10 \times 10^6$  cells per 150-mm cell-culture dish (day 1). The following day (day 2), cells were transfected with the calcium phosphate method. On day 3, transfected cells were transferred at 15,000 to 20,000 cells per well in 50  $\mu$ l of medium into poly-L-lysine-coated and rinsed 384-well white, clear-bottomed cell-culture plates (Greiner Bio-One). On day 4, 3.5 $\times$  drug stimulation solutions were prepared in filter-sterilized assay buffer, which consisted of 20 mM HEPES and 1 $\times$  HBSS, pH 7.4, and 20  $\mu$ l was added to each well. On day 5, medium and drug solutions were removed from the wells (by aspiration or shaking), and 20  $\mu$ l per well of Bright-Glo solution (Promega) diluted 20-fold in assay buffer was added to each well. After incubation for 15–20 min at room temperature, luminescence was counted in a Trilux luminescence counter. Results in the form of relative luminescence units (RLU) were exported into Excel spreadsheets, and GraphPad Prism was used for analysis of data. To measure constitutive activity, no ligand was added on day 4.

**PRESTO-Tango GPCRome screening  $\beta$ -arrestin-recruitment assay.** Details of this assay are described in **Supplementary Note 2**.

**Immunofluorescence.** On day 1, cells (15,000/well in 384-well clear-bottomed, black plates) were prefixed with 4% paraformaldehyde (PFA) for 30 min at RT, incubated with anti-Flag antibody (1:500, polyclonal rabbit anti-Flag, Sigma, F1804), and incubated for 1 h at room temperature and then overnight at 4 °C. On day 2, cells were incubated with Alexa Fluor 594-conjugated goat anti-rabbit antibody (1:200, Invitrogen, A-11012) and nuclear dye (Hoechst 33342, 1:2,000, Invitrogen) for 1 h at RT in the dark. After thorough washing with PBS (1 $\times$  PBS, 0.5 mM CaCl<sub>2</sub>, pH 7.4), cells were postfixed with 4% PFA for 30 min on ice and stored at 4 °C in the dark. Images were obtained with the BD Pathway Bioimaging System (BD).

**PI hydrolysis.** HEK293T cells were maintained in DMEM supplemented with 10% FBS, 100 U/ml penicillin and 100  $\mu$ g/ml streptomycin. Cells were transfected with 10  $\mu$ g of receptor DNA per 15-cm cell-culture dish and incubated overnight at 37 °C in a humidified 5% CO<sub>2</sub> incubator; the next day, cells were seeded into poly-L-lysine-coated 96-well plates in 200  $\mu$ l per well of DMEM supplemented with 1% dialyzed FBS, 100 U/ml penicillin and 100  $\mu$ g/ml streptomycin. After

attaching to the plate, cells were incubated for 16 h as above in inositol-free DMEM (United States Biological) containing 1% dialyzed FBS, and 1  $\mu$ Ci/well of [<sup>3</sup>H]inositol. Next, cells were washed with 100  $\mu$ l drug buffer (1 $\times$  HBSS, 24 mM NaHCO<sub>3</sub>, 11 mM glucose, and 15 mM LiCl, pH 7.4) and treated with 100  $\mu$ l of drug buffer containing 10  $\mu$ M drug in quadruplicate for 1 h at 37 °C in a 5% CO<sub>2</sub> incubator. Alternatively, for concentration-response curves, cells were treated with a range of concentrations in quadruplicate in 100  $\mu$ l of drug buffer and incubated for 1 h at 37 °C in a 5% CO<sub>2</sub> incubator. After treatment, drug solution was removed, and 40  $\mu$ l of 50 mM formic acid was added to lyse cells for 30 min at 4 °C. After cell lysis, 40  $\mu$ l of acid extracts was transferred to a polyethylene terephthalate 96-well sample plate (PerkinElmer, 1450-401) and mixed with 75  $\mu$ l of PerkinElmer RNA Binding YSi SPA Beads (RPNQ0013) at a concentration of 0.2 mg beads/well and incubated for 30 min at 4 °C. Bead/lysate mixtures were then counted with a PerkinElmer 2450 MicroPlate Counter.

**Ca<sup>2+</sup>-mobilization assay.** Cells were plated (15,000 cells/well) into poly-L-lysine-coated 384-well clear-bottomed, black-walled microplates (Greiner Bio-One) with 40  $\mu$ l of medium (DMEM supplemented with 500  $\mu$ g/ml geneticin sulfate (G-418), 1% dialyzed FBS, and 50 U of penicillin/50  $\mu$ g of streptomycin) and incubated overnight (37 °C, 5% CO<sub>2</sub>). The following day, medium was replaced with 20  $\mu$ l of calcium dye (FLIPR Calcium 4 Assay Kit; Molecular Devices) diluted in assay buffer (1 $\times$  HBSS, 2.5 mM probenecid, and 20 mM HEPES, pH 7.4–7.8) and incubated for 45 min at 37 °C and 15 min at room temperature. Compounds were initially dissolved in DMSO at 10 mM. The 16-point curves were prepared as 3 $\times$  serial dilutions for each compound, with final concentrations ranging from 10  $\mu$ M to 0.003 nM. Basal fluorescence was measured for 10 s, then 10  $\mu$ l of test or control compounds were added, and this was followed by continued fluorescence measurement for an additional 120 s. Raw data were plotted as a function of molar concentration of test compound with Prism 5.0 (GraphPad Software).

**Generation of stable cell lines.** Inducible cell lines expressing MRGPRX1, MRGPRX2 or MRGPRX4 were generated with the Flp-In T-Rex Core Kit (Invitrogen) according to the manufacturer's instructions. In brief, genes were subcloned into the pcDNA5/FRT/TO vector and cotransfected with the POG44 expression plasmid into the Flp-In T-Rex HEK-T cell line with FuGENE HD transfection reagent (Promega). Receptor-expressing cells were selected and maintained in DMEM containing 10% FBS, 15  $\mu$ g/ml blasticidin, 100  $\mu$ g/ml hygromycin B, and 100 U penicillin and 100  $\mu$ g/ml streptomycin. Receptor expression after 24 h of 1  $\mu$ g/ml tetracycline treatment was confirmed via immunofluorescence with an anti-Flag antibody (Sigma, F1804) as above.

50. Jordan, M., Schallhorn, A. & Wurm, F.M. Transfecting mammalian cells: optimization of critical parameters affecting calcium-phosphate precipitate formation. *Nucleic Acids Res.* **24**, 596–601 (1996).